Development of flow and efficiency characteristics of an axial compressor with an analytical method including cooling air extraction and variable inlet guide vane angle

PAWEŁ TRAWIŃSKI[*]

Institute of Heat Engineering, Warsaw University of Technology,
Nowowiejska 21/25, 00-665, Warsaw, Poland

Abstract   The development of a reliable mathematical model of an axial compressor requires applying flow and efficiency characteristics. This approach provides performance parameters of a machine depending on varying conditions. In this paper, a method for developing characteristics of an axial compressor is presented, based on general compressor maps available in the literature or measurement data from industrial facilities. The novelty that constitutes the core of this article is introducing an improved method describing the performance lines of an axial compressor with the modified ellipse equation. The proposed model is extended with bleed air extraction for the purposes of cooling the blades in the expander part of the gas turbine. The variable inlet guide vanes angle is also considered using the vane angle correction factor. All developed dependencies are fully analytical. The presented approach does not require knowledge of machine geometry. The set of input parameters is based on reference data. The presented approach makes it possible to determine the allowed operating area and study the machine's performance in variable conditions. The introduced mathematical correlations provide a fully analytical study of optimum operating points concerning the chosen criterion. The final section presents a mathematical model of an axial compressor built using the developed method. A detailed study of the exemplary flow and efficiency characteristics of an axial compressor operating with a gas turbine is also provided.

Keywords: Axial compressor; Compressor characteristics; Compressor maps; IGV; Bleed air

[*]Corresponding Author. Email: ptraw@itc.pw.edu.pl

Nomenclature

A, B	–	semi axes of ellipse
a_0, a_1, a_2, a_3, a_4	–	coefficients of approximation function for surge line
e	–	Euler's number
IGV	–	inlet guide vane
k	–	auxiliary constant for internal cooling model
$k_{A1}, k_{A2}, k_{B1}, k_{B2}$	–	additional coefficients of modified ellipse equation
MRE	–	mean relative error
m	–	mass flow
n	–	rotational speed
p	–	pressure
R	–	coefficient of correlation
RMSE	–	root mean squared error
SF	–	safety factor
T	–	temperature
VACF	–	vane angle correction factor
v	–	displacement vector
x, y	–	Cartesian coordinates

Greek symbols

α	–	clockwise angle of rotation
Δ	–	increment
η	–	efficiency
θ	–	coefficient of temperature ratio
π	–	pressure ratio
φ	–	mass flow ratio

Subscripts

0	–	center point
air	–	atmospheric air
amb	–	ambient conditions
blade	–	gas turbine blade
cool	–	internal cooling
exh	–	exhaust gases
film	–	film cooling
in	–	inlet
min	–	minimum value
max	–	maximum value
nom	–	nominal parameter
red	–	reduced parameter
rot	–	rotated coordinate system
surge	–	surge line
total	–	total value
v	–	displaced coordinate system

1 Introduction

The axial compressor is one of the main components included in a gas turbine unit. A reliable modelling and accurate representation of the performance of an axial compressor is possible using individual flow and efficiency characteristics. However, this data is hardly available because manufacturers do not provide detailed specification defining the operation of the machine to public knowledge. Furthermore, the data provided by manufacturers may not be applicable for a unit that has been operating for a considerable time and its performance has deteriorated. Commercial engineering software does not have fully developed tools in this area either. One of the alternatives to this state of matter is the usage and adaptation of general maps available in the literature [1, 2].

The technological progress in the development of gas turbine systems resulted in axial compressors being highly advanced units. This provides a challenge in designing reliable and precise mathematical models. Increasing the flexibility of gas turbine unit performance and improving its efficiency across a more comprehensive load range became possible by introducing movable blades of the first or several first nozzle rows [3, 4]. In turn, the aim to maximise the power and efficiency of the system is achieved, among other possibilities, by increasing the inlet temperature to the expansion section of the gas turbine unit [5]. However, this requires advanced cooling systems using bleed air from the compressor part [2, 6]. The discussed aspects should be considered in the development of the mathematical model of the system and the use of general maps of axial compressors.

This paper presents a method of mathematical description and implementation of general maps of an axial compressor in a mathematical model of a gas turbine system. The lines of operation are characterised by the equation of an ellipse. Attempts to use a similar approach can occasionally be found in the subject literature [7, 8]. The novelty of the presented approach is the possibility of arbitrary displacement and rotation of ellipses describing the operating lines and dependence of characteristic values of the ellipse upon reduced parameters defining the operation of the axial compressor. Additionally, the proposed model is extended by including bleed air intake for blade cooling in the expansion section of the gas turbine unit. Moreover, the effect of variable inlet guide vane (IGV) angle is also considered using the vane angle correction factor (VACF). All the developed dependencies are fully analytical. This approach allows visualising the relationships between the axial compressor performance parameters and fully

understanding their influence on the machine operation. Obtaining such an interpretation can be difficult or even impossible using empirical functions.

In the final part of the article, exemplary calculations for an axial compressor model that is a part of a gas turbine unit are presented. The created computer programme is a reflection of the developed mathematical relationships. The axial compressor model cooperates with the combustion chamber and the expansion part of the gas turbine unit. The generated results allow investigating the influence of various factors (mainly ambient temperature and the degree of opening of the first nozzle row) on the machine performance. In particular, the achieved pressure ratio, the axial compressor's internal efficiency and the total fraction of the air cooling the blades in the expansion part of the turbine set are analysed. The conducted study enables identification of the points of optimum machine operation depending on external conditions.

2   General map of an axial compressor

The general maps of axial compressors are widely available in [4, 9–11]. They are developed based on dimensionless analysis, which uses reduced parameters. It allows comparing the performance of machines with similar geometry and analysing the performance of a particular compressor under different than nominal conditions. Using reduced parameters implies the reference of the current operating conditions of the machine to nominal values [2]. The essential reduced parameters include:

- reduced pressure ratio

$$\pi_{\text{red}} = \frac{\pi}{\pi_{\text{nom}}}\,, \tag{1}$$

- reduced rotational speed

$$n_{\text{red}} = \frac{n}{n_{\text{nom}}} \sqrt{\frac{(T_{\text{in}})_{\text{nom}}}{T_{\text{in}}}}\,, \tag{2}$$

- reduced mass flow

$$\varphi_{\text{red}} = \frac{\dot{m}}{\dot{m}_{\text{nom}}} \frac{(p_{\text{in}})_{\text{nom}}}{p_{\text{in}}} \sqrt{\frac{T_{\text{in}}}{(T_{\text{in}})_{\text{nom}}}}\,, \tag{3}$$

- reduced internal efficiency

$$\eta_{\text{red}} = \frac{\eta}{\eta_{\text{nom}}} \, . \tag{4}$$

The general map of the axial compressor is usually given in reduced pressure ratio, π_{red}, and reduced inlet mass flow, φ_{red}. Typically it includes two sets of data. The first dataset contains the lines of constant reduced rotational speed, n_{red}, it is a flow characteristic. The second dataset regards the lines of constant reduced internal efficiency, η_{red}, it is an efficiency characteristic. These characteristics are commonly presented on a unified plot. Unambiguous determination of the operating point of an axial compressor is possible, assuming the knowledge of ambient conditions, values of nominal machine parameters and inlet airflow [2].

Determining the performance of an axial compressor using the general maps should start with calculating the reduced values of mass flow, φ_{red}, and the rotational speed, n_{red}. Then, using the flow characteristic, the point on the constant line of reduced rotational speed, n_{red}, that corresponds to the value of the reduced mass flow, φ_{red}, is found – it indicates the value of the reduced pressure ratio, π_{red}. In the last step, the efficiency characteristic should be used, on which it is necessary to find the line of reduced internal efficiency, η_{red}, crossing the point determined by the values of the reduced parameters of mass flow, φ_{red}, and pressure ratio, π_{red}.

The allowable operating area of an axial compressor is limited on one side by the surge line. It indicates the maximum outlet pressure above which pumping occurs in operation. This phenomenon is hazardous and undesirable during machine performance. In practice, during load operation of a compressor, the lower limit is mostly the maximum volumetric flow of the medium resulting from the geometry of the flow system.

The lines of constant reduced rotational speed, n_{red}, and constant reduced internal efficiency, η_{red}, resemble an ellipse. Attempts of mathematical description of the indicated characteristics using the ellipse equation can be found in the literature [7,8]. However, most of them are founded on the basic ellipse equation with constant parameters and central point set in the origin of the coordinate system. In the following part of this paper, the equation of an ellipse moved freely about the centre of the coordinate system and rotated by an arbitrary angle is discussed.

For the purpose of implementation of the developed model, the general maps given in [2] were selected. The presented data refer to the group of

stages of the power compressor. The plot was digitalised. Detailed data can be found in Fig. 1 and the further part of this publication.
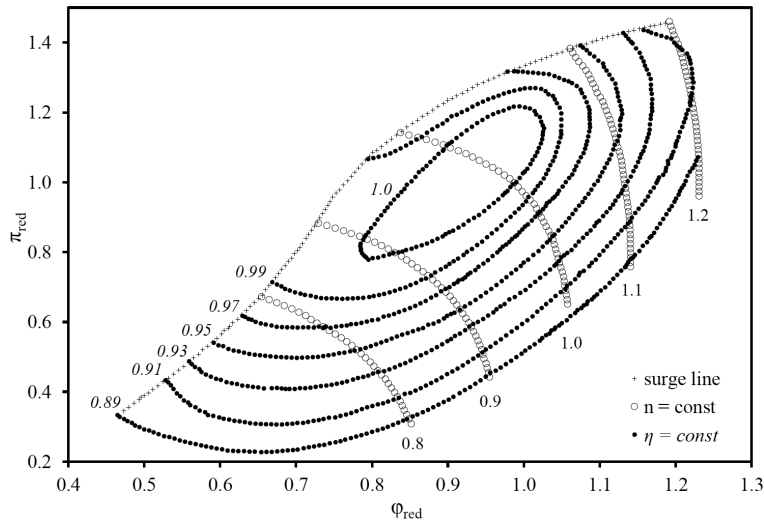

Figure 1: The digitised general map of an axial compressor [2].

3 Equation of an ellipse

Consideration of selecting a suitable model equation began with an analysis of the fundamental equation of an ellipse with A and B semi-axes along the axis of the coordinate system and central point at the origin of the coordinate system [12]

$$\frac{x^2}{A^2} + \frac{y^2}{B^2} = 1. \tag{5}$$

In the subsequent step, the possibility of free displacement of the ellipse regarding the origin of the coordinate system by the vector v was added [12]

$$v = [x_0, y_0]. \tag{6}$$

The study of the displacement vector led to determining the relationship between the original and displaced coordinate systems

$$\begin{bmatrix} x_v \\ y_v \end{bmatrix} = \begin{bmatrix} x \\ y \end{bmatrix} + \begin{bmatrix} x_0 \\ y_0 \end{bmatrix}. \tag{7}$$

From the matrix notation (7), it was possible to identify the correlations for the individual coordinates in the new coordinate system:

$$x_v = x + x_0 \,, \tag{8}$$

$$y_v = y + y_0 \,. \tag{9}$$

The final step was to add the possibility of rotating the ellipse by an arbitrary angle α in the clockwise direction. The inclusion of rotation also required defining the relationship between the original and rotated coordinate systems. The most convenient way was the matrix notation [12]

$$\begin{bmatrix} x_{\text{rot}} \\ y_{\text{rot}} \end{bmatrix} = \begin{bmatrix} \cos\alpha & \sin\alpha \\ -\sin\alpha & \cos\alpha \end{bmatrix} \begin{bmatrix} x \\ y \end{bmatrix}. \tag{10}$$

Deriving the particular relations for the coordinates in the rotated coordinate system resulted in the following dependencies:

$$x_{\text{rot}} = x\cos\alpha + y\sin\alpha, \tag{11}$$

$$y_{\text{rot}} = y\cos\alpha - x\sin\alpha. \tag{12}$$

Due to the linear nature of the transformations associated with displacement and rotation, the order in which they were applied to the ellipse equation was irrelevant. However, it should be noted that if the rotation of the ellipse is applied first, the displacement vector v also has to be rotated. Considering relations (7) to (12) in Eq. (5) resulted in obtaining the general equation of the displaced and rotated ellipse. The relation

$$\frac{(x\cos\alpha - y\sin\alpha - x_0)^2}{A^2} + \frac{(x\sin\alpha + y\cos\alpha - y_0)^2}{B^2} = 1 \,. \tag{13}$$

was used to describe the lines of constant reduced rotational speed, n_{red}, and constant reduced internal efficiency, η_{red}. The algorithm detailed in [13] was used to obtain the constants present in the ellipse equation (13). The method allows the best fitting of the ellipse to a set of given points using the least-squares method. The calculation of the characteristic values is performed directly analytically without the iterative process. The method is marked by simplicity, stability and ease of implementation in the form of computational code.

4   Limiting lines

The construction of the mathematical model of the general maps of the compressor began with the description of the lines limiting the allowed operating area. As pointed out earlier, the critical from the point of view of machine operation is the surge line, which defines the maximum allowed reduced pressure ratio, π_{red}, for a given reduced mass flow, φ_{red}, at the compressor inlet. In the process of digitising the plot, 126 points in the range of the reduced mass flow, φ_{red}, from 0.4659 to 1.1869 were obtained. This range is sufficient considering the most typical range of compressor exploitation. The relation

$$\pi_{\mathrm{surge}} = a_0 e^{\varphi_{\mathrm{red}}} + a_1 \varphi_{\mathrm{red}} + a_2 \varphi_{\mathrm{red}}^2 + a_3 \varphi_{\mathrm{red}}^3 + a_4 \varphi_{\mathrm{red}}^4 \qquad (14)$$

was applied to interpolate the obtained points. The coefficients of the interpolation polynomial were determined by the least-squares method. The coefficient of determination was $R^2 = 99.987\%$, the root mean squared error RMSE $= 0.0114$. The summary and coefficients of the interpolation polynomial are summarised in Table 1. Obtained course of surge line is presented in Fig. 2.
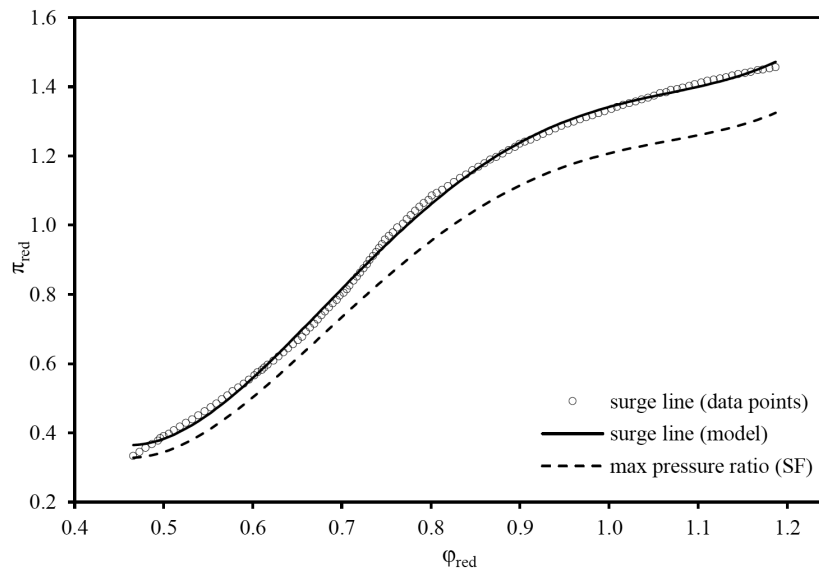

Figure 2: Surge line – general compressor map data and implemented model.

Table 1: Summary and coefficients of the interpolation polynomial in Eq. (14).

Number of data points	126		a_0	6.971873631
$\min \varphi_{\mathrm{red}}$	0.466		a_1	−45.16569164
$\max \varphi_{\mathrm{red}}$	1.187	Coefficients	a_2	72.68927847
R^2	99.987		a_3	−62.08593611
RMSE	0.0114		a_4	16.95228178

Due to the safety and stability of axial compressor operation, it was decided to introduce an additional variable, including the safety factor as

$$\pi_{\max} = (1 - \mathrm{SF}_{\mathrm{surge}}) \, \pi_{\mathrm{surge}} \,. \tag{15}$$

The value of the safety factor was assumed as $\mathrm{SF}_{\mathrm{surge}} = 0.15$.

5 Lines of constant reduced rotational speed

The flow characteristic defines the relationship between the reduced parameters: pressure ratio π_{red}, mass flow, φ_{red}, and rotational speed, n_{red}. For the analysis, the lines of constant reduced rotational speed n_{red} corresponding to the values: 0.8, 0.9, 1.0, 1.1, and 1.2 were selected. This range is adequate for a broad spectrum of operation of an axial power compressor. A total of 205 points were obtained by digitising the general plot. For the mathematical description of constant reduced rotational speed lines, two equations based on the ellipse Eq. (13) were proposed, which can be written in the general form

$$\frac{(\varphi_{\mathrm{red}} \cos \alpha - \pi_{\mathrm{red}} \sin \alpha - \varphi_0)^2}{A^2} + \frac{(\varphi_{\mathrm{red}} \sin \alpha + \pi_{\mathrm{red}} \cos \alpha - \pi_0)^2}{B^2} = 1 \,. \tag{16}$$

5.1 Simplified model

For each of the data series corresponding to successive values of the reduced rotational speed n_{red}, the algorithm given in [13] was applied to calculate the characteristic values of the fitted ellipse. In this way, a set of five equations for a family of ellipses was obtained, which described the relationship between the reduced values of the pressure ratio, π_{red}, and the mass flow, φ_{red}, for successive values of the reduced rotational speed, n_{red}. Each of the obtained equations was represented by individual values of selected characteristic parameters of the ellipse: φ_0, π_0, α, A, B – Fig. 3.
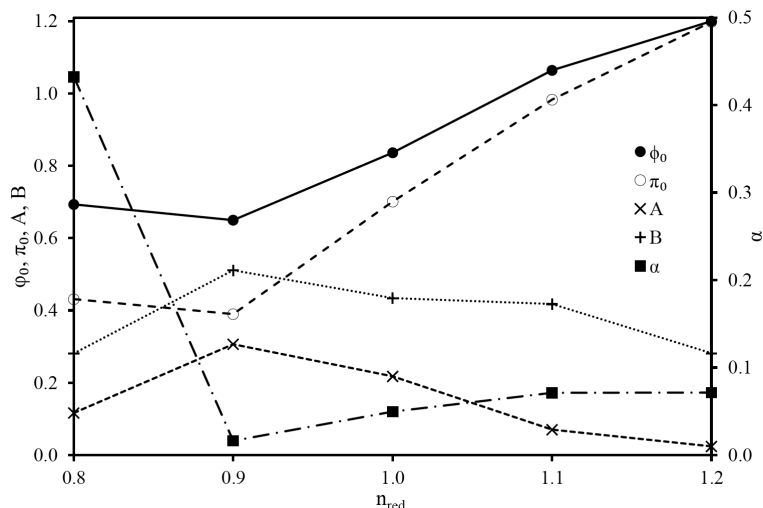
Figure 3: Characteristic values of the ellipses obtained in the simplified model of the flow characteristics.

Due to high variability and non-monotonic course of points indicating characteristic values of ellipses, it was decided to apply approximation with linear functions for values of n_{red} located inside intervals between analysed series. Interpolation using polynomials resulted in a significant instability of the obtained functions inside the intervals between given points of n_{red}.

5.2 Complex model

In fact, the shapes of lines of the constant reduced rotational speed, n_{red}, do not represent ideal ellipses. In the complex model, it was decided to introduce additional functions parameterising the characteristic values A and B with respect to the value of the reduced mass flow, φ_{red}:

$$A = A_0 + k_{A1}\varphi_{red} + k_{A2}\varphi_{red}^2 , \tag{17}$$

$$B = B_0 + k_{B1}\varphi_{red} + k_{B2}\varphi_{red}^2 . \tag{18}$$

Further optimisation of the model equation was carried out by minimising the RMSE using the nonlinear generalized reduced gradient (GRG) method [14]. The initial parameters for the optimisation problem were the values obtained in the simplified model. During the minimisation of the objective function, all the characteristic values of the ellipse φ_0, π_0, α and

additionally introduced parameters A_0, B_0, k_{A1}, k_{A2}, k_{B1}, k_{B2} were adjusted anew – Figs. 4 and 5. Similarly, as in the simplified model, due to the large variability of values of the obtained parameters, it was decided to apply approximation with linear functions inside the intervals between the analysed values of the reduced rotational speed, n_{red}.
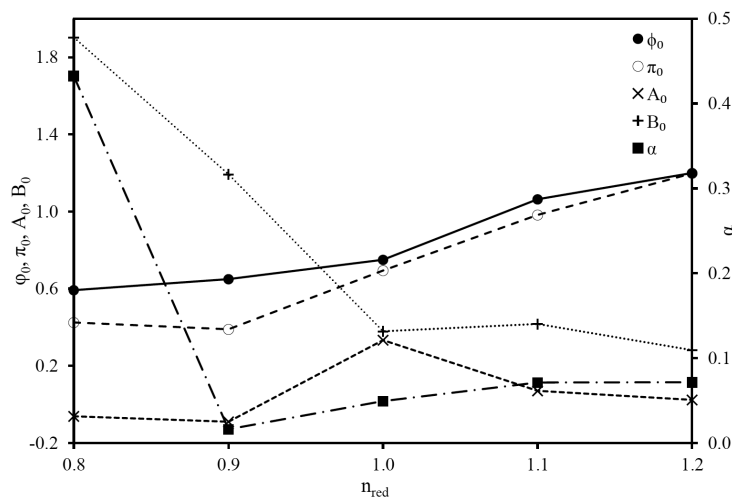

Figure 4: Characteristic values: φ_0, π_0, A_0, B_0, and α of the ellipses obtained in the complex model of flow characteristics.
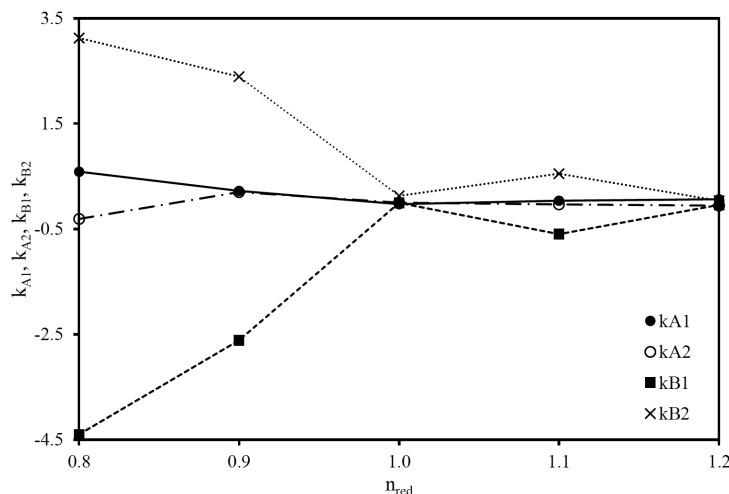

Figure 5: Values of the additional parameters k_{A1}, k_{A2}, k_{B1}, and k_{B2} of the ellipses obtained in the complex model of flow characteristics.

5.3 Model comparison

The obtained mathematical models describing the flow characteristics were found to have very good representativeness of the data. In the case of the simplified model, the coefficient of determination, R^2, was 99.04%, taking into account all series of reduced rotational speed, n_{red}. The simplified model was noticeably losing accuracy with the increase of the reduced rotational speed, n_{red}, as reflected by the increase in mean relative error (MRE) and RMSE values and the decrease in the value of the coefficient of determination R^2. It was caused by the shape of the consecutive lines of $n_{red} = $ const, which significantly depart from the ellipse's shape for larger values of this parameter. In the case of the complex model, the introduction of additional parameterisation of the A and B semi-axes contributed to a better representation of the examined flow characteristics – Fig. 6. In this case, for the entire range of data, the coefficient of determination R^2 was 99.66%.
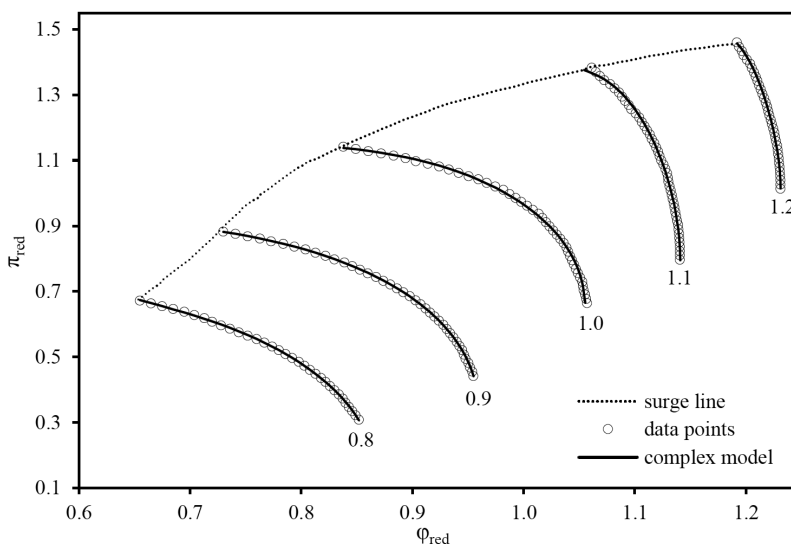

Figure 6: Flow characteristics of an axial compressor using a complex model.

Notably, the introduction of additional dependencies for the A and B semi-axes improved the model's accuracy for the range of higher values of the reduced rotational speed, n_{red}. The difference was particularly identifiable for the last dataset of $n_{red} = 1.2$, where the value of the coefficient of deter-

mination R^2 for the complex model was 99.01% compared with 96.65% for the simplified model. The summary of the obtained results of the developed mathematical models is presented in Table 2.

Table 2: Comparison of simplified and complex model for flow characteristics.

Reduced rotational speed, η_{red}	Number of data points	MRE $\times 10^{-3}$		RMSE $\times 10^{-2}$		R^2	
		simplified	complex	simplified	complex	simplified	complex
0.8	33	-0.796	-0.001	0.638	1.475	0.9966	0.9998
0.9	40	-0.189	0.009	0.263	1.456	0.9996	0.9999
1.0	44	1.850	0.001	7.928	0.703	0.9972	0.9978
1.1	49	4.526	0.603	15.419	1.003	0.9930	0.9971
1.2	39	10.620	0.723	2.710	1.472	0.9665	0.9901
Total	205	3.335	0.284	6.057	1.192	0.9904	0.9966

6 Lines of constant reduced efficiency

The efficiency characteristic of an axial compressor defines the relationship between the reduced parameters: pressure ratio, π_{red}, mass flow, φ_{red}, and internal efficiency, η_{red}. The construction of the mathematical model was based on all the lines of constant reduced internal efficiency, η_{red}, available on the general map, which included the values: 0.89, 0.91, 0.93, 0.95, 0.97, 0.99, and 1.0. In this case, the coverage of the analysis was also entirely sufficient to represent the compressor performance over a broad operating spectrum and primarily covered the most common load region. Digitisation of the general map produced a total of 881 points for seven data series. Based on the ellipse equation (13), two model equations were proposed for the mathematical description of the constant reduced internal efficiency lines. The general form of the studied relationships was identical to that of the flow characteristic (16).

6.1 Simplified model

The datasets describing the lines of constant internal efficiency, η_{red}, were analysed by an algorithm implemented based on [13]. It allowed obtaining characteristic values for each of the fitted ellipses. In this way, a set of seven equations describing the family of ellipses relating the reduced values

of the pressure ratio, π_{red}, and the mass flow, φ_{red}, for successive values
of the reduced internal efficiency, η_{red}, was obtained. Each of the resulting
equations contained individually adjusted values of characteristic parame-
ters of the ellipse: φ_0, π_0, α, A, B – Fig. 7. As in the flow characteristic
model, the values of characteristic parameters inside the intervals defined
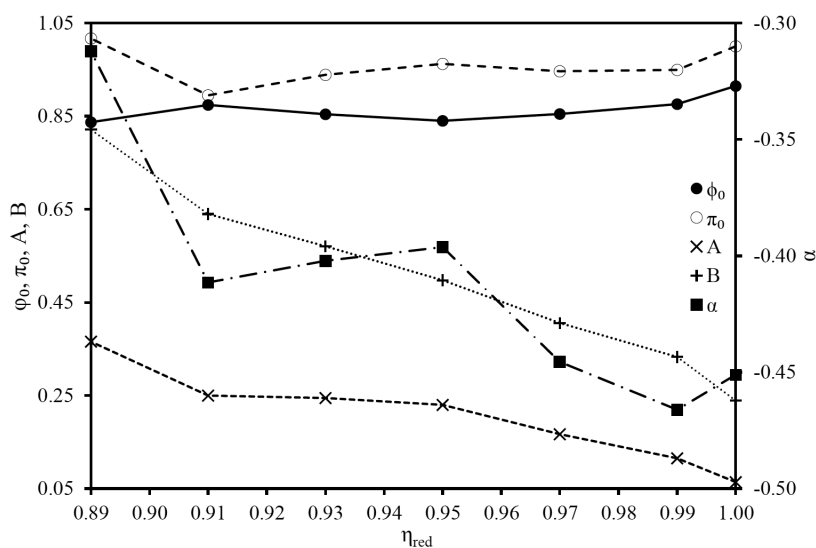by the dataset points were approximated by linear functions.

Figure 7: Characteristic values of the ellipses obtained in the simplified
model of the efficiency characteristics.

6.2   Complex model

The distances between the obtained ellipse centres and the farthest points
along the A and B semi-axes were, in fact, not equal, which may be no-
ticed in Fig. 1. The complex model was extended by introducing additional
functions depending on the characteristic values of A and B of ellipses with
the value of the reduced mass flow, φ_{red}. The general forms of equations
were as in (17) and (18). Further optimisation of the complex model pro-
ceeded analogously to the calculations related to the flow characteristics.
As a result, the parameter sets: φ_0, π_0, α, A_0, B_0, k_{A1}, k_{A2}, k_{B1}, and k_{B2}
were obtained for all data series covering the analysed values of the reduced
internal efficiency, η_{red} – Figs. 8 and 9.
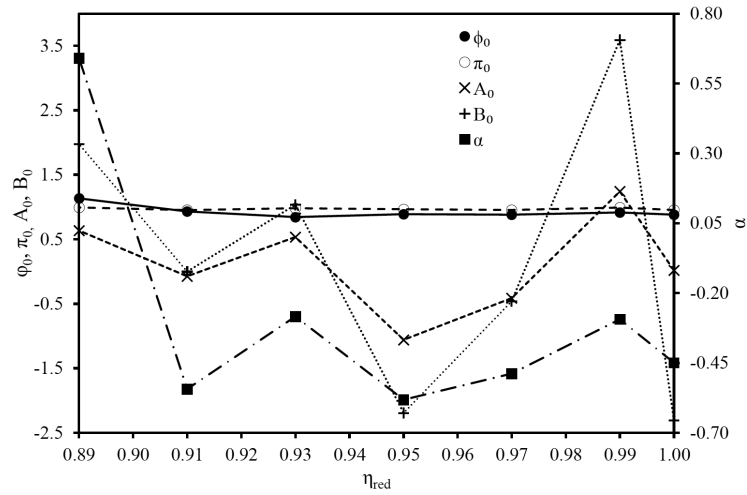
Figure 8: Characteristic values φ_0, π_0, A_0, B_0, and α of the ellipses obtained in the complex model of efficiency characteristics.
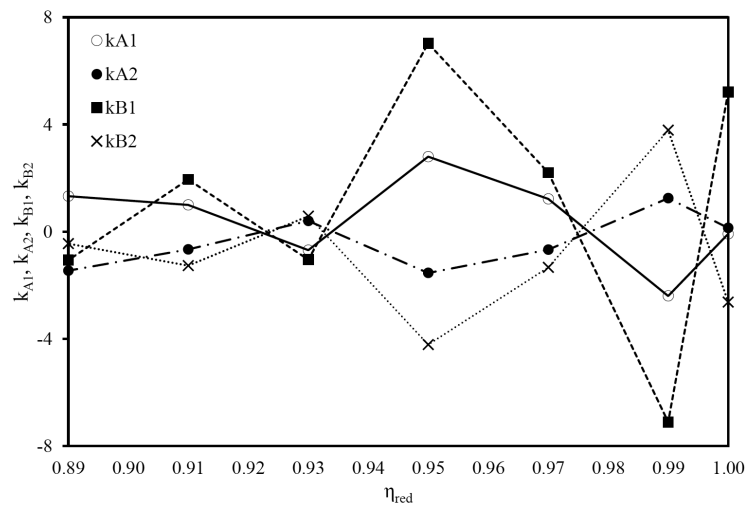

Figure 9: Values of the additional parameters k_{A1}, k_{A2}, k_{B1}, and k_{B2} of the ellipses obtained in the complex model of efficiency characteristics.

6.3   Model comparison

The developed mathematical models of the efficiency characteristics were able to represent the analysed data precisely. The simplified model achieved a coefficient of determination, R^2, of 99.80%, including all constant reduced

internal efficiency datasets. The accuracy of this model decreased with an
increasing value of η_{red}. The least accurate area was the range of maximum
reduced internal efficiency $\eta_{red} = 1.0$, for which the coefficient of determi-
nation, R^2,was 98.95%. It was caused by the irregular shape of the curve,
which remarkably deviated from an ellipse. The introduction of additional
parameterisation of characteristic values A and B significantly enhanced
the model fit in the entire range of the general map – Fig. 10. The complex
model achieved a coefficient of determination R^2 of 99.94% for all series
of reduced internal efficiency. The fit in the region of maximum reduced
internal efficiency $\eta_{red} = 1.0$ was equally high; the model explained 99.43%
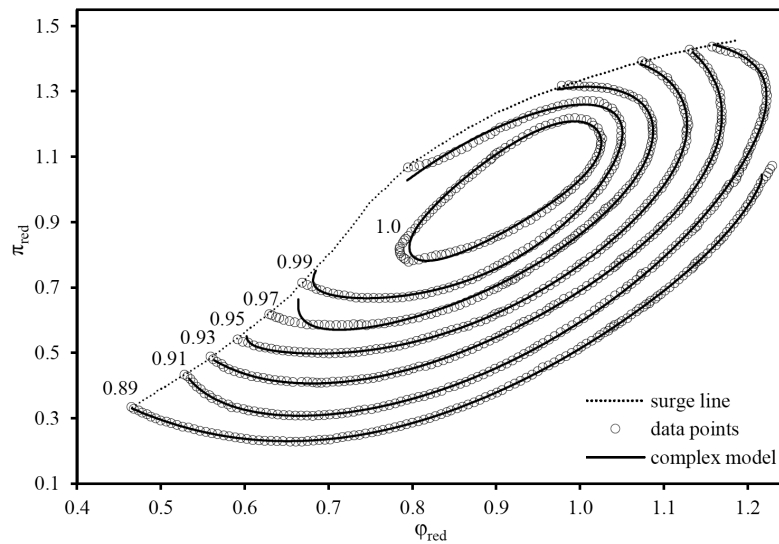of the variability of the parameters.

Figure 10: Efficiency characteristics of an axial compressor using a complex
model.

As it can be noticed in Fig. 10, the developed mathematical models of the ef-
ficiency characteristics performed least successfully for values of $\eta_{red} = 0.97$
and $\eta_{red} = 0.99$ nearby the surge line. However, further studies reduced this
area after considering the safety factor, SF_{surge}, for the maximum reduced
pressure ratio, π_{max}. A summary of the results of the developed mathemat-
ical models is given in Table 3.

Table 3: Comparison of simplified and complex model for efficiency characteristics.

Reduced rotational speed, η_{red}	Number of data points	MRE $\times 10^{-3}$		RMSE $\times 10^{-2}$		R^2	
		simplified	complex	simplified	complex	simplified	complex
1.00	104	0.719	0.001	1.438	1.058	0.9895	0.9943
0.99	113	−2.283	0.000	1.587	0.837	0.9948	0.9985
0.97	119	0.250	−0.002	0.960	0.947	0.9986	0.9986
0.95	116	1.901	−0.013	0.953	0.478	0.9989	0.9997
0.93	134	0.643	−0.012	0.973	0.433	0.9991	0.9998
0.91	155	−0.877	0.154	1.852	0.524	0.9976	0.9998
0.89	140	0.045	0.000	0.502	0.261	0.9996	0.9999
Total	881	0.027	0.023	1.182	0.623	0.9980	0.9994

7 Impact of variable inlet guide vanes angle

Movable blades of the first stage of the compressor provide increased flexibility in the operation of the gas turbine system and improve the unit's efficiency over a wide performance range. The variable angle of the IGVs changes the geometry of the machine flow system. Considering this when analysing unit performance should be reflected in the development and adjustment of general compressor characteristics. The inclusion of the variable IGVs angle in the equations describing the relationships between the reduced parameters of pressure ratio, π_{red}, and mass flow, φ_{red}, was possible through the use of the parameter VACF, which expresses the percentage change in the mass flow of the inlet air with respect to the change in the position of the first stage guide vanes

$$\text{VACF} = \frac{\dot{m}_{max} - \dot{m}_{min}}{\dot{m}_{max} \left(\text{IGV}_{max} - \text{IGV}_{min} \right)} \,. \tag{19}$$

For power compressors, the value of the VACF parameter oscillates around 1% [1].

According to [1], changing the IGVs angle affects only the flow characteristics of the axial compressor. The inclusion of the parameter does not modify the shape of the lines of constant reduced rotational speed, n_{red}; it only leads to a displacement of the characteristics along the horizontal axis of the coordinate system.

The actual mass flow rate of the compressor's inlet air with the VACF parameter can be written in the general form

$$\dot{m} = \dot{m}_{\max} \left[1 - \text{VACF} \left(\text{IGV}_{\max} - \text{IGV} \right) \right]. \tag{20}$$

The difference between the maximum mass flow rate of the inlet air entering the compressor and the current value can be written in the general form

$$\frac{\Delta \dot{m}_{\text{IGV}}}{\dot{m}_{\max}} = \text{VACF} \left(\text{IGV}_{\max} - \text{IGV} \right). \tag{21}$$

Relating this difference to the nominal values of the machine resulted in the expression for the reduced mass flow loss (22) due to flow throttling at the compressor inlet

$$\Delta \varphi_{\text{IGV}} = \text{VACF} \left(\text{IGV}_{\max} - \text{IGV} \right) \frac{(p_{\text{in}})_{\text{nom}}}{p_{\text{in}}} \sqrt{\frac{T_{\text{in}}}{(T_{\text{in}})_{\text{nom}}}}. \tag{22}$$

The value of the parameter $\Delta \varphi_{IGV}$ specifies the displacement of the compressor flow characteristics along the plot's horizontal axis. The transformation is linear and can be included in model Eq. (16), similarly to the displacement by a vector (6). An example of the effect of changing the IGVs angle on the obtained general characteristics is presented in Fig. 11.
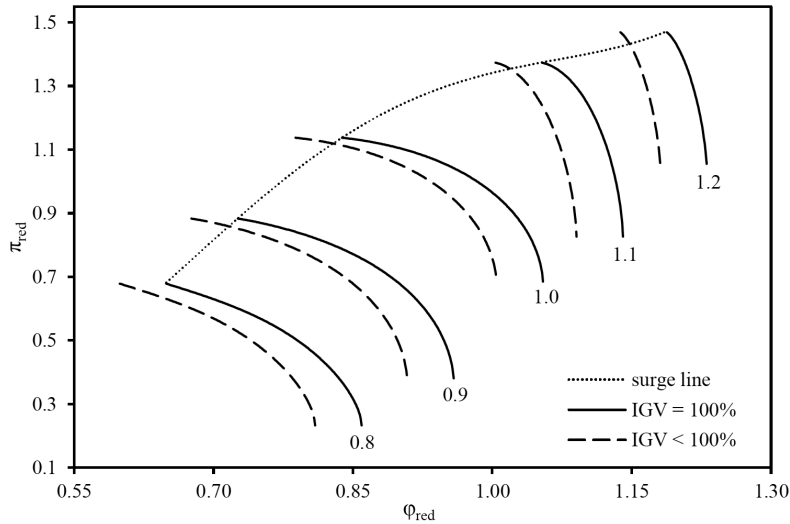

Figure 11: Effect of compressor first stage blades closure on flow characteristics.

8 Impact of bleed air intake

A systematic attempt to maximise the efficiency of gas turbine units is realised, among other possibilities, by raising the inlet temperature to the expansion section. The first stages of the turbine operate in the presence of a working medium with a temperature significantly exceeding the material durability of possible metal alloys, even with the application of an additional thermal barrier coating (TBC) [4,6]. It necessitates the introduction of additional technological solutions in the form of advanced cooling systems for the blade rows with air extracted from the compressor bleeds [2]. Consideration of the cooling air intake should be included in the analysis of the unit's performance.

The correlation between the gas turbine inlet temperature and the total demand for cooling air extracted from the compressor bleeds related to the inlet mass flow is approximately a linear function [15]. Interpolation of the data available in the literature for an inlet temperature of 1500°C provided an estimated value of the fraction of cooling air at the level of 20.9% – Fig. 12.

It was assumed that the presence of compressor bleeds does not affect the shape of the general flow and efficiency characteristics. The increase in the compressor inlet flow due to additional cooling intake moved the
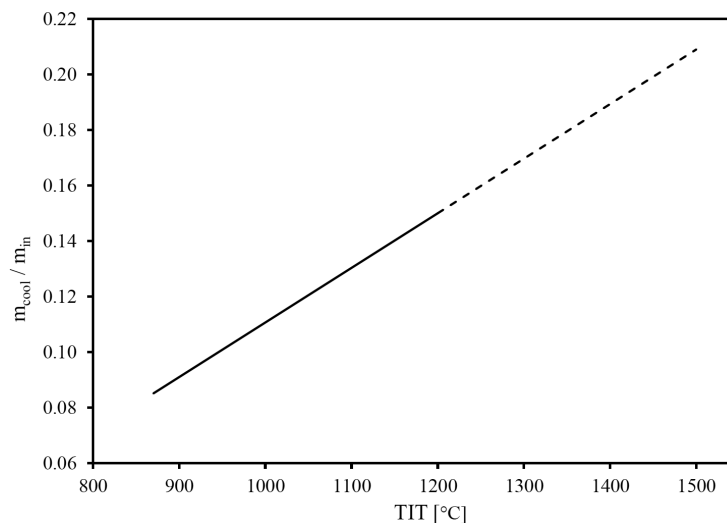

Figure 12: The total fraction of bleed air for cooling the stages of the expansion section with respect to the turbine inlet temperature (TIT) [15].

current operating point of the machine on the characteristics following the change in the reduced mass flow rate, φ_{red}. Determination of the amount of cooling air was based on the detailed model of the air film cooling process presented in [6]. Only the essential dependencies enabling calculation of the mass flow rate of the bleed air necessary to ensure the required cooling of the rows in the expansion section were presented.

According to the literature data [6], the air film cooling efficiency was assumed as $\varepsilon_{\mathrm{film}} = 0.4$, while the cooling process efficiency was assumed as $\eta_{\mathrm{cool}} = 0.7$. The required total cooling efficiency of the blades, $\varepsilon_{\mathrm{total}}$, was expressed as the relationship between the temperature of the exhaust gases T_{exh}, the cooling air from the compressor bleed T_{air} and the allowable metal temperature of blades T_{blade}

$$\varepsilon_{\mathrm{total}} = \frac{T_{\mathrm{exh}} - T_{\mathrm{blade}}}{T_{\mathrm{exh}} - T_{\mathrm{air}}} \,. \tag{23}$$

The temperature difference ratio, θ, for the air film cooling process was given by

$$\theta = \frac{\varepsilon_{\mathrm{total}} \left(1 - \eta_{\mathrm{cool}}\right) \varepsilon_{\mathrm{film}} - \varepsilon_{\mathrm{total}}\varepsilon_{\mathrm{film}}\eta_{\mathrm{cool}}}{\eta_{\mathrm{cool}} \left(1 - \varepsilon_{\mathrm{total}}\right)} \,. \tag{24}$$

Introducing an additional constant $k_{\mathrm{cool}} = 0.03$ characterising the parameters related to the flow of the working medium and the geometry of the blade system [6], and a safety factor $\mathrm{SF}_{\mathrm{cool}} = 1.5$, the equation expressing the fraction of the mass flow of the cooling air in relation to the total mass flow of the exhaust gases at the turbine stage inlet can be written as

$$\frac{\dot{m}_{\mathrm{cool}}}{\dot{m}_{\mathrm{exh}}} = \mathrm{SF}_{\mathrm{cool}}k_{\mathrm{cool}}\theta \,. \tag{25}$$

The obtained analytical equation determines the mass flows of bleed air for cooling the expansion part of the turbine unit as a function of the allowable temperature of turbine blades, T_{blade}, and the temperatures of working mediums: exhaust gases, T_{exh}, and cooling air, T_{air}.

9   Mathematical model of an axial compressor

Based on the formulated dependencies, a computational programme simulating the operation of an axial compressor was developed. The mathematical model of the working medium was implemented based on [16] using the Redlich-Kwong real gas equation of state. Calculations for the compressor

flow system were carried out using the stage-stacking method. The model considered the general flow and efficiency characteristics, the possibility of changing the IGVs angle and the air intake from the compressor bleeds for cooling the rows of the expansion section of the gas turbine.

The modelled axial compressor unit cooperated with the combustion chamber and expander. The flow system of the axial compressor had 17 stages. The nominal atmospheric air parameters at the machine inlet corresponded to normal conditions. Adjusting the flow rate at the inlet to the system was possible due to the variable IGVs angle of the first nozzle row ranging from $-20°$ to $15°$. The combustion chamber ensured a constant exhaust gas temperature of $1500°$C at the expander inlet. The expansion section of the turbine consisted of four stages, the first three of which were cooled by air from the compressor system. The fourth stage did not require additional cooling. The allowable temperature of the expander blades was $T_{\text{blade}} = 770°$C. The first compressor bleed was located after the 10th stage and supplied air to the third expander nozzle row, the second bleed was located after the 14th stage and supplied air to the second nozzle row. Furthermore, part of the air from the compressor outlet was taken for cooling purposes: the first nozzle and rotor rows, the second and third rotor rows. It should be pointed out that the conducted analysis concerned only the operation of the axial compressor model. It did not include the variable parameters of operation of the combustion chamber and the expansion part of the gas turbine unit. The allowable blade temperature in the expansion section and the exhaust gas temperatures at the inlet to the specific turbine stages, which were only used to determine the bleed air flows for cooling purposes, were assumed to be constant and unchanged with the gas turbine unit load. Therefore, only the results concerning the compressor part of the gas turbine unit were presented in the following section. The assumptions of the axial compressor model are summarised in Table 4. Additional assumptions for the cooling system can be found in Table 5.

Table 4: Assumptions for the mathematical model of the axial compressor.

Parameter	Value	Unit	Parameter	Value	Unit
Number of stages	17	–	m_{nom}	680	kg/s
T_{nom}	15	°C	η_{max}	93	%
p_{nom}	101.325	kPa	IGVs range	35	°
π_{nom}	21	–	VACF	1	%

Table 5: Assumptions for the cooling of the expander blades system.

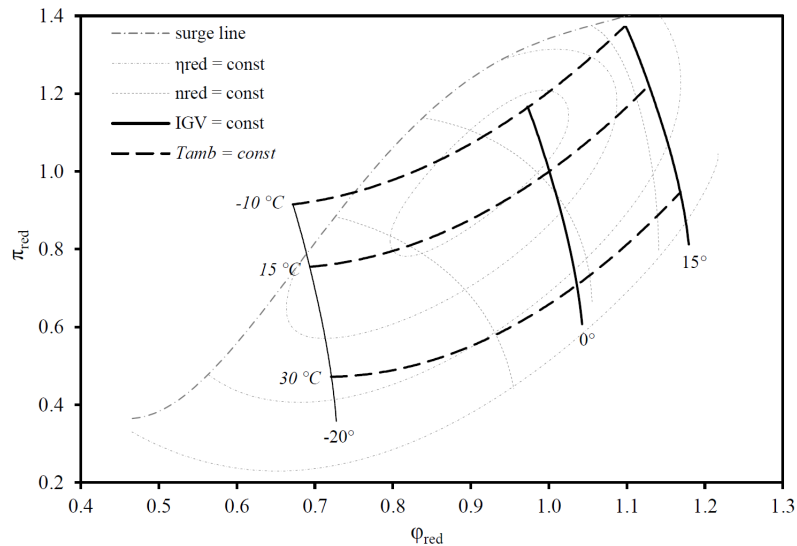| Turbine row	Exhaust gas inlet $^\circ$C	Cooling air from compressor system
1. nozzle	1500	outlet
1. rotor	1360	outlet
2. nozzle	1240	14. stage
2. rotor	1130	outlet
3. nozzle	1030	10. stage
3. rotor	930	outlet

10   Results

The performance of the mathematical model of the axial compressor was studied mainly in terms of the influence of the ambient air temperature and the IGVs angle. Only the operation of the gas turbine unit at nominal rotational speed was considered.

For extreme ambient air temperatures, the obtained values of reduced rotational speed ranged from $n_{\mathrm{red}} = 0.967$ (for $T_{\max} = 35^\circ$C) to $n_{\mathrm{red}} = 1.046$ (for $T_{\min} = -10^\circ$C). As mentioned in Section 5, the mapped area of the general flow characteristic (from $n_{\mathrm{red}} = 0.8$ to $n_{\mathrm{red}} = 1.2$) for operation at nominal rotational speed was comprehensive. Inverse calculations using Eq. (2) indicated that the range from $n_{\mathrm{red}} = 0.9$ to $n_{\mathrm{red}} = 1.1$ covered the region of ambient air temperatures from $T_{\min} = -35.0^\circ$C to $T_{\max} = 82.6^\circ$C. Therefore, for issues related to the operation of the axial compressor at synchronous speed, it is possible to narrow the area of the flow characteristics model. Detailed data obtained from the mathematical model of the axial compressor for various values of the IGVs angle and inlet temperature, T_{amb}, are presented in Table 6. Assuming and selecting input data sets for the model considered the allowable operating area of the machine.

The inclusion of the parameters characterising the geometry of the compressor blade system and the range of adjustment of the inlet angle provided flow and efficiency characteristics regarding the ambient temperature, T_{amb}, and the actual IGVs angle. The operation lines corresponding to $T_{\mathrm{amb}} = $ const and IGV $= $ const with the parameters established for the mathematical model in Table 4 are presented in Fig. 13. The operation lines were superimposed on the general compressor map obtained earlier in this paper.

Table 6: Detailed data obtained from the mathematical model of the axial compressor.

IGV angle	°	−20			0			15		
Inlet air temperature	°C	10	15	30	−10	15	30	−10	15	20
Discharge pressure	MPa	2.16	2.03	1.44	2.62	2.03	1.44	2.62	2.03	1.88
Compressor efficiency	%	92.1	92.6	92.1	91.8	92.3	85.6	89.4	85.3	83.7
Compressor power	MW	239.3	234.7	209.5	306.6	294.6	285.9	363.9	372.5	373.5
Cooling air extraction after 10. stage	pressure	MPa	0.83	0.79	0.61	0.97	0.79	0.61	0.97	0.79	0.75
	temperature	°C	259.2	259.3	246.4	246.2	260.1	262.2	252.5	279.1	283.1
	mass flow	kg/s	6.3	6.3	6.1	7.6	7.9	8.0	8.9	9.7	9.8
Cooling air extraction after 14. stage	pressure	MPa	1.49	1.41	1.03	1.78	1.41	1.03	1.78	1.41	1.31
	temperature	°C	359.6	357.5	333.6	349.8	358.8	358.4	360.0	388.9	393.3
	mass flow	kg/s	18.1	18.0	16.9	22.0	22.6	22.6	26.0	28.1	28.5
Cooling air from outlet	pressure	MPa	2.19	2.05	1.46	2.65	2.05	1.46	2.65	2.05	1.90
	temperature	°C	434.9	431.0	399.1	427.6	432.7	431.7	441.1	472.6	477.5
	mass flow	kg/s	84.5	83.5	76.0	103.4	104.9	104.6	123.9	136.9	139.1
Total cooling air	kg/s	108.9	107.8	99.1	133.0	135.4	135.1	158.8	174.7	177.4
	%	20.0	19.8	18.2	19.6	19.9	19.9	20.3	22.3	22.7

Figure 13: Operation lines for T_{amb} = const and IGV = const obtained
for the mathematical model of the axial compressor.

The course of the operation lines for a constant opening of IGVs was characterised by a greater slope angle than for the lines of constant reduced rotational speed, $n_{\text{red}} = \text{const}$. The shape of the obtained characteristics corresponded to similar data in literature sources, e.g. [2]. On the entire length of the line representing a given opening $\text{IGV} = \text{const}$, there was a constant flow of the inlet air. The upper ends of the $\text{IGV} = \text{const}$ curves, corresponding to lower air temperatures, were moved towards lower values of φ_{red}. The lower ends of the $\text{IGV} = \text{const}$ curves, corresponding to higher air temperatures, were moved towards higher values of φ_{red}. For a constant inlet flow, the reduced mass flow rate was lower for lower temperatures and higher for higher temperatures. Moreover, a relationship can be observed between the achieved reduced pressure ratio, π_{red}, and the inlet temperature T_{amb} – the higher the inlet temperature, the lower the achieved reduced pressure ratio. This dependence can be explained based on the course of lines of constant reduced rotational speed, n_{red}. First of all, the higher the inlet air temperature, T_{amb}, the higher the reduced mass flow rate, as noted above. An analysis of the constant reduced rotational speed lines n_{red} indicated that for higher values of reduced mass flow rate, a lower reduced pressure ratio, π_{red}, was achieved. Furthermore, higher temperatures correspond to lower values of the reduced rotational speed. For lower values of the reduced rotational speed, the flow characteristic lines are located in the area of the lower achievable reduced pressure ratios. It is worth noting that for the adopted parameters defining the compressor geometry and its nominal values, it was possible to go beyond the allowable exploitation area of the machine indicated by the surge line.

The influence of the opening angle of IGVs on the internal efficiency, η, of the axial compressor at a constant inlet temperature, T_{amb}, is shown in Fig. 14. The course of the operating lines resulted directly from the combination of the flow and efficiency characteristics. Each curve for a constant ambient temperature T_{amb} was characterised by an optimum compressor operating point, depending on the IGVs opening angle. As the inlet temperature decreased, the optimum operating point moved towards higher degree of opening of the inlet guide vanes.

The influence of the inlet temperature, T_{amb}, on the internal efficiency, η, of the axial compressor at a constant opening angle of IGVs is shown in Fig. 15. As in the previous case, the course of the compressor operating curves followed directly from the flow-efficiency characteristics. Each of the curves for a constant opening degree of IGVs was characterised by a point of optimum machine operation. The IGVs opening degree affected the shape
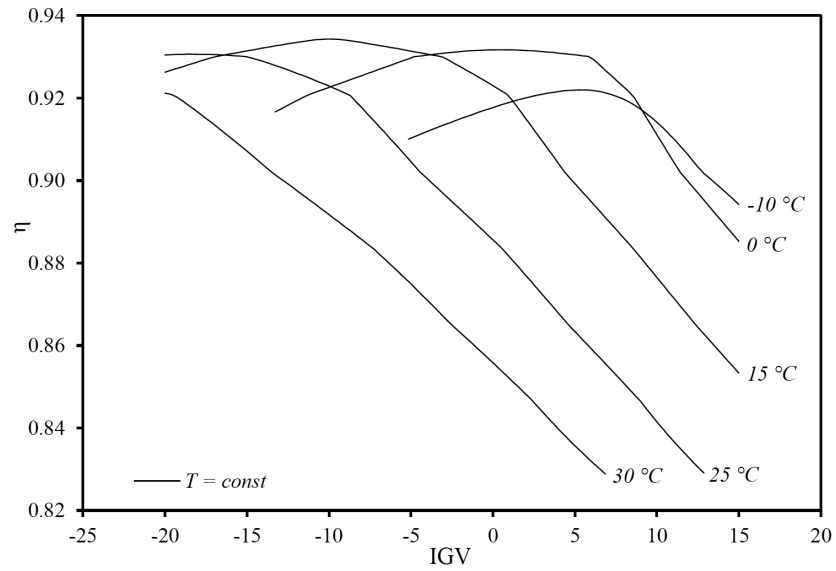
Figure 14: Influence of the IGVs angle on the internal efficiency of the axial compressor.
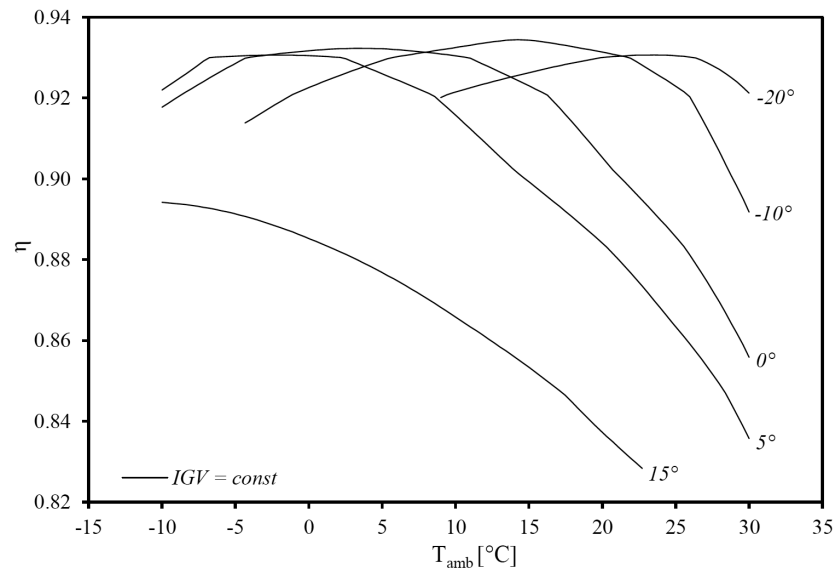

Figure 15: Influence of the inlet temperature, T_{amb}, on the internal efficiency of the axial compressor.

of the performance curves and moved the optimum operating point towards lower inlet temperatures.

The opening angle of IGVs and the inlet temperature, T_{amb}, have a noticeable influence on the performance of the axial compressor. The knowledge of the flow and efficiency characteristics and the resulting operational curves allows identifying the optimal operating point of the machine unequivocally. A detailed analysis of the achieved operating curves provides the information required to plan the exploitation of the compressor in the most efficient way. It is also possible to find the allowable operating area of a compressor concerning the actual ambient conditions.

The total fraction of bleed air for the cooling of the expansion part of the turbine system related to the compressor inlet flow as a function of ambient air temperature is shown in Fig. 16. The obtained curves refer to the minimum, nominal and maximum opening angle of the IGV.
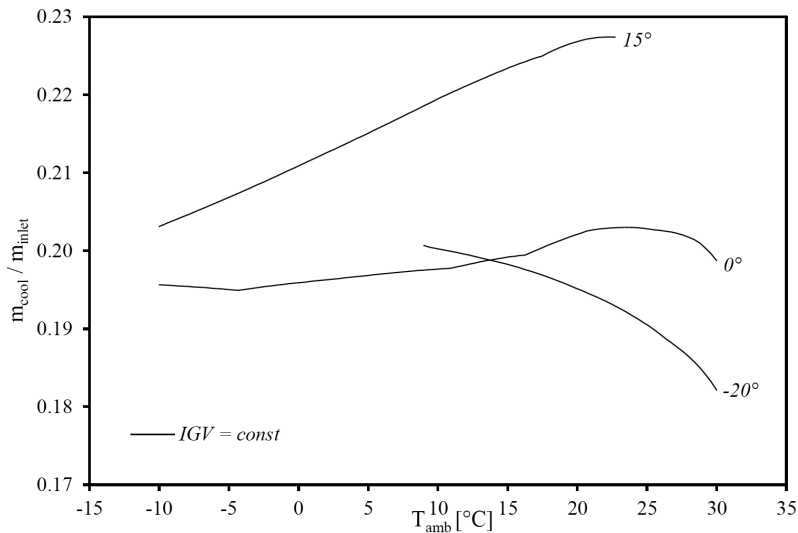

Figure 16: Influence of inlet temperature, T_{amb}, on the cooling air fraction.

The total fraction of bleed air for the cooling of the expansion part of the turbine system related to the compressor inlet flow as a function of IGVs opening is shown in Fig. 17. The obtained curves refer to three exemplary ambient air temperatures.

The indication of correlations between the total fraction of cooling air, the inlet air temperature and the degree of opening of the first nozzle row was not clear. As pointed out in the previous part of this publication, the
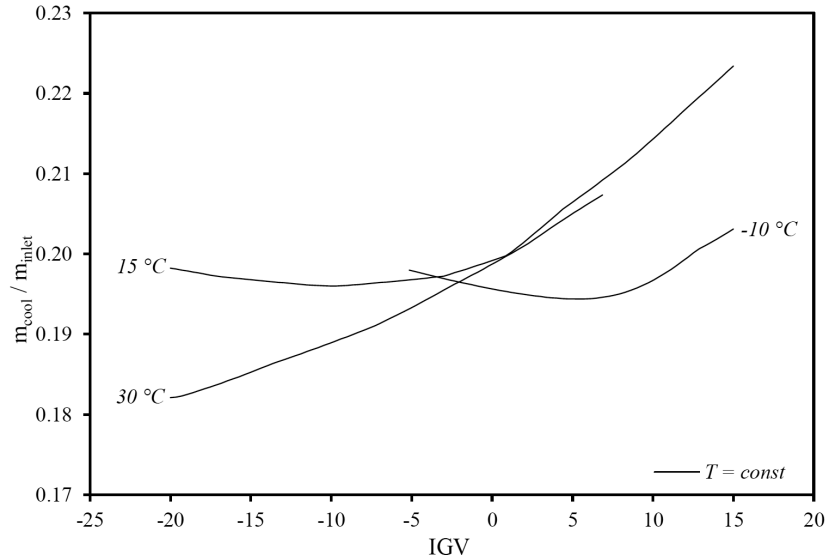
Figure 17: Influence of IGVs opening angle on cooling air fraction.

amount of cooling air depended mainly on the temperature coefficient θ – Eq. (25). Assuming constant temperatures in the exhaust gas path in the gas turbine section, T_{exh}, (Table 5) and allowable blade temperature, T_{blade}, the only variable was the air temperature in the control profiles of the axial compressor, T_{air}. This temperature depended on two parameters: the achieved pressure ratio and the internal efficiency of the axial compressor.

As mentioned in the previous section, the pressure ratio achievable in an axial compressor depended on the ambient temperature – the lower the temperature, the higher the pressure ratio. An increase in pressure ratio translated directly into an increase in temperatures in the control profiles of the unit (bleed and discharge ports). As the bleed air temperature increased, it was necessary to supply more air for cooling the expansion section so that the blade metal temperature remained constant. There was also a clear correlation between the total fraction of cooling air and the internal efficiency of the axial compressor – Fig. 18. As the efficiency of the machine increased, the demand for bleed air decreased. An increase in internal efficiency translated into a decrease in temperatures across the flow profile of the compressor. As the bleed air temperatures decreased, the air required for cooling while maintaining the allowable blade metal temperature constant was reduced.
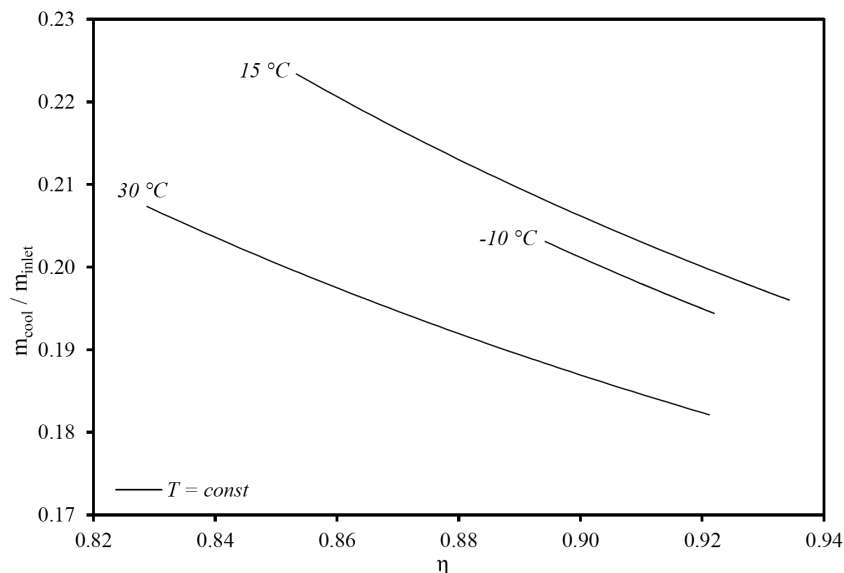
Figure 18: Influence of internal efficiency and ambient temperature, T_{amb}, on the cooling air fraction.

11 Summary and conclusions

This paper presented a method for the mathematical description of the general flow and efficiency characteristics of an axial compressor using a modified ellipse equation. The models known from the literature were extended by the possibility of free displacement of ellipses and rotation towards a coordinate system. Moreover, the characteristic values of the obtained families of ellipses were related to the reduced parameters of the axial compressor in the simplified approach: for the flow characteristics – to the reduced rotational speed, n_{red}, for the efficiency characteristics – to the reduced internal efficiency, η_{red}. Additional dependencies for the semi-axes A and B in relation to the reduced mass flow, φ_{red}, were introduced for the complex model. Both proposed models – simplified and complex – of the description of the general maps were marked by a high coefficient of determination R^2, which indicated an accurate representation of the original datasets. Application of the model extended by additional functions, especially for efficiency characteristics – due to their irregular course, improved the accuracy of the mathematical description in the broader area of machine performance. The course of the obtained operational lines was more precise and accurate

compared to the results provided by the simplified ellipse equation [7, 8].

The implemented compressor model also included a set of dependencies expressing the influence of the variable IGVs angle. The mathematical description of this phenomenon was based on the VACF coefficient, which expresses the percentage change of the air inlet flow in relation to the change of the IGVs angle. An additional parameter enabled to determine the compressor flow characteristic displacement resulting from a change in the geometry of the flow system. The modelled system was extended by considering the extraction of the compressor bleed air to cool the blades in the expansion part of the turbine unit. The description of the phenomenon was based on the relationships defining the air film cooling process, which is used in advanced systems with gas turbines.

The prepared set of relationships was implemented in the form of a computer programme simulating the performance of an axial compressor cooperating with a gas turbine unit. As a result, it was possible to study the system's behaviour across varying input conditions – primarily the inlet temperature and the opening IGVs angle. The applied relationships are fully analytical, resulting in a computationally inexpensive exploration of optimal exploitation scenarios.

The description of axial compressor operation with general maps brings several advantages, among which the most important is that no detailed knowledge of machine geometry is required. Using nominal and reduced parameters is sufficient. Such a universal approach enables coverage of any multistage power compressor. The flow and efficiency characteristics provide an easy way to visualise the operating point of the unit, which may be very useful for potential usage by operating personnel in an industrial plant. Also, the lines limiting the allowed exploitation area of the machine can be read from the generated maps. The proposed approach can be successfully used in developing calculation models of systems with multistage axial compressors. A mathematical model of a compressor based on the described approach can be an attractive diagnostic tool for industrial applications. It is also possible to analyse machine degradation and loss of performance parameters. Moreover, the presented algorithm can create individual characteristics based on actual measurement data from industrial facilities.

References

[1] Plis M.: *Mathematical modeling of an axial compressor in a gas turbine system.* J. Power Technol. **96**(2016), 3, 194–199.

[2] Badyda K., Miller A.: *Power Gas Turbines and Systems with Their Application.* Kaprint, Lublin 2014 (in Polish).

[3] Kehlhofer R., Rukes B., Hennemann F., Stirnimann F.: *Combined-Cycle Gas and Steam Turbine Power Plants.* PennWell, Tusla 2009.

[4] Boyce M.P.: *Gas Turbine Engineering Handbook.* Butterworth-Heinemann, Houston 2011.

[5] Kotowicz J.: *The current state and prospects of development of gas-steam systems.* Arch. Energ. **42**(2012), 1 23–28, (in Polish).

[6] Horlock J.H.: *Advanced Gas Turbine Cycles.* Pergamon, Kidlington 2013.

[7] Tsoutsanis E., Li Y. G., Pilidis P., Newby M.: *Part-load performance of gas turbines: Part I: – A novel compr/essor map generation approach suitable for adaptive simulation.* In: Proc. ASME Gas Turbine India Conf., Mumbai, 1 Dec. 2012, GTINDIA2012-9580, 733–742.

[8] Tsoutsanis E., Meskin N., Benammar M., Khashayar K.: *A component map tuning method for performance prediction and diagnostics of gas turbine compressors.* Appl. Energ. **135**(2014), 572–585,.

[9] Giampaolo A.J.: *Gas Turbine Handbook: Principles and Practices.* Fairmont CRC / Taylor&Francis, Lilburn Boca Raton 2006.

[10] Eckert B.: *Axial and Radial Compressors.* PWT, Warszawa 1959 (in Polish).

[11] Saravanamuttoo H.I.H.: *Gas Turbine Theory.* Pearson/Prentice Hall, Harlow 2009.

[12] Kalman D.: *The most marvelous theorem in mathematics.* J. Online Math. Appl. **8**(2008).

[13] Halir R., Flusser J.: *Numerically stable direct least squares fitting of ellipses.* In: Proc. 6th Int. Conf. Central Europe on Computer Graphics and Visualization, Plzen, 1998, 125–132

[14] https://www.solver.com/excel-solver-grg-nonlinear-solving-method-stopping-conditions (accessed 27 May 2021).

[15] Perycz S.: *Steam and Gas Turbines.* Ossolineum, Wydawn. IMP PAN, Wrocław 1992 (in Polish).

[16] Trawiński P.: *Development of real gas model operating in gas turbine system in Python programming environment.* Arch. Thermodyn. **41**(2020), 4, 23–61.